Vimentin Knockdown Decreases Corneal Opacity

Subrata K. Das,[1] Isha Gupta,[1] Yang Kyung Cho,[2] Xiaohui Zhang,[1] Hironori Uehara,[1] Santosh Kumar Muddana,[1] Ashlie A. Bernhisel,[1] Bonnie Archer,[1] and Balamurali K. Ambati[1]

[1]Department of Ophthalmology, Moran Eye Center, University of Utah, Salt Lake City, Utah, United States
[2]St. Vincent's Hospital, College of Medicine, The Catholic University of Korea, Suwon, South Korea

Correspondence: Balamurali K. Ambati, Moran Eye Center, University of Utah, 65 Mario Capecchi Drive, Salt Lake City, UT 84132, USA; Bala.ambati@utah.edu.

Submitted: October 22, 2013
Accepted: May 5, 2014

Citation: Das SK, Gupta I, Cho YK, et al. Vimentin knockdown decreases corneal opacity. *Invest Ophthalmol Vis Sci*. 2014;55:4030–4040. DOI:10.1167/iovs.13-13494

Purpose. Wound induced corneal fibrosis can lead to permanent visual impairment. Keratocyte activation and differentiation play a key role in fibrosis, and vimentin, a major structural type III intermediate filament, is a required component of this process. The purpose of our study was to develop a nonviral therapeutic strategy for treating corneal fibrosis in which we targeted the knockdown of vimentin.

Methods. To determine the duration of plasmid expression in corneal keratocytes, we injected a naked plasmid expressing green fluorescent protein (GFP; pCMV-GFP) into an unwounded mouse corneal stroma. We then injected pCMV-GFP or plasmids expressing small hairpin RNA in the corneal wound injury model (full-thickness corneal incision) to evaluate opacification.

Results. GFP expression peaked between days 1 and 3 and had prominent expression for 15 days. In the corneal wound injury model, we found that the GFP-positive cells demonstrated extensive dendritic-like processes that extended to adjacent cells, whereas the vimentin knockdown model showed significantly reduced corneal opacity.

Conclusions. These findings suggest that a nonviral gene therapeutic approach has potential for treating corneal fibrosis and ultimately reducing scarring.

Keywords: corneal fibroblasts, corneal wound healing, keratocytes

Corneal fibrosis and the resulting opacity is the third leading cause of blindness worldwide.[1,2] Corneal fibrosis often results from infection, refractive surgery complications, chemical burns, and traumatic eye injury.[3–5] Photorefractive keratectomy (PRK) is a popular laser eye surgery aimed at correcting visual refractive errors[6,7]; however, despite recent increased success of postoperative outcomes in PRK, corneal fibrosis and opacity remain major complications of this procedure. Several treatments have been proposed to reverse the resultant corneal disruption, including topical steroids, cell cycle inhibitors (mitomycin-C), urokinase-type plasminogen activators, and interferon α-2b. Currently, these pharmacological treatments are limited by ineffectiveness or an undesirable side effect profile.[29–32]

Gene therapy provides a novel mode with which to treat ocular surface disorders such as corneal fibrosis. The cornea is an attractive location for gene therapy because of its accessibility, immune-privileged status, and simplicity of monitoring treatment. Various viral and nonviral vectors have been used to deliver gene therapy to the cornea.[8–13] For example, gene therapy has been used to effectively deliver vascular endothelial growth factor (VEGF) cDNA to the corneal stroma.[12] Although delivery of viral vectors provides increased transfection efficiency compared to a nonviral strategy, these vectors tend to induce an inflammatory response that often results in adverse side effects.[14–16] Therefore, in corneal fibrosis, nonviral gene therapy is an attractive option for treatment.

The molecular mechanism of corneal fibrosis has been studied extensively. In corneal injury, the keratocytes of the stroma become activated and migrate to the wound site and often transform into fibroblasts.[17–21] Subsequently, some of these fibroblasts further differentiate into myofibroblasts, which synthesize and secrete extracellular matrix (ECM) that is then incorporated into an intricate meshwork that promotes wound contracture. This tightening of the meshwork often manifests as corneal opacity that compromises corneal clarity and vision. Vimentin is a major structural intermediate filament (type III) protein expressed in fibroblasts[22] and in low levels in normal corneal keratocytes.[23–25] However, following injury, vimentin is overexpressed in the stroma at the site of injury as it provides the forces required for wound contracture.[26–28] Furthermore, it may play a role in cell migration after injury, as demonstrated by a study that shows vimentin-deficient mice having delayed migration of fibroblasts to the wound site as a result of reduced mechanical stability of the ECM.[23,24]

In this study, we sought to determine whether vimentin knockdown by an intracorneal short hairpin RNA (shRNA) plasmid injection could reduce corneal fibrosis and opacity in an in vivo corneal injury model.

Methods

Plasmid

The plasmid vector pCMV-GFP was made from pCMV-Script (Agilent Technology, Santa Clara, CA, USA) in our laboratory. Antisense plasmid against vimentin (pshRNA.vim) and 1 nonspecific shRNA plasmid (pshRNA.neg) were made into pSilencer 4.1-CMV neo (Life Technologies, Carlsbad, CA, USA) according to the manufacturer's instructions. Plasmids grown in *Escherichia coli* host strain were purified using the endotoxin-

Copyright 2014 The Association for Research in Vision and Ophthalmology, Inc.

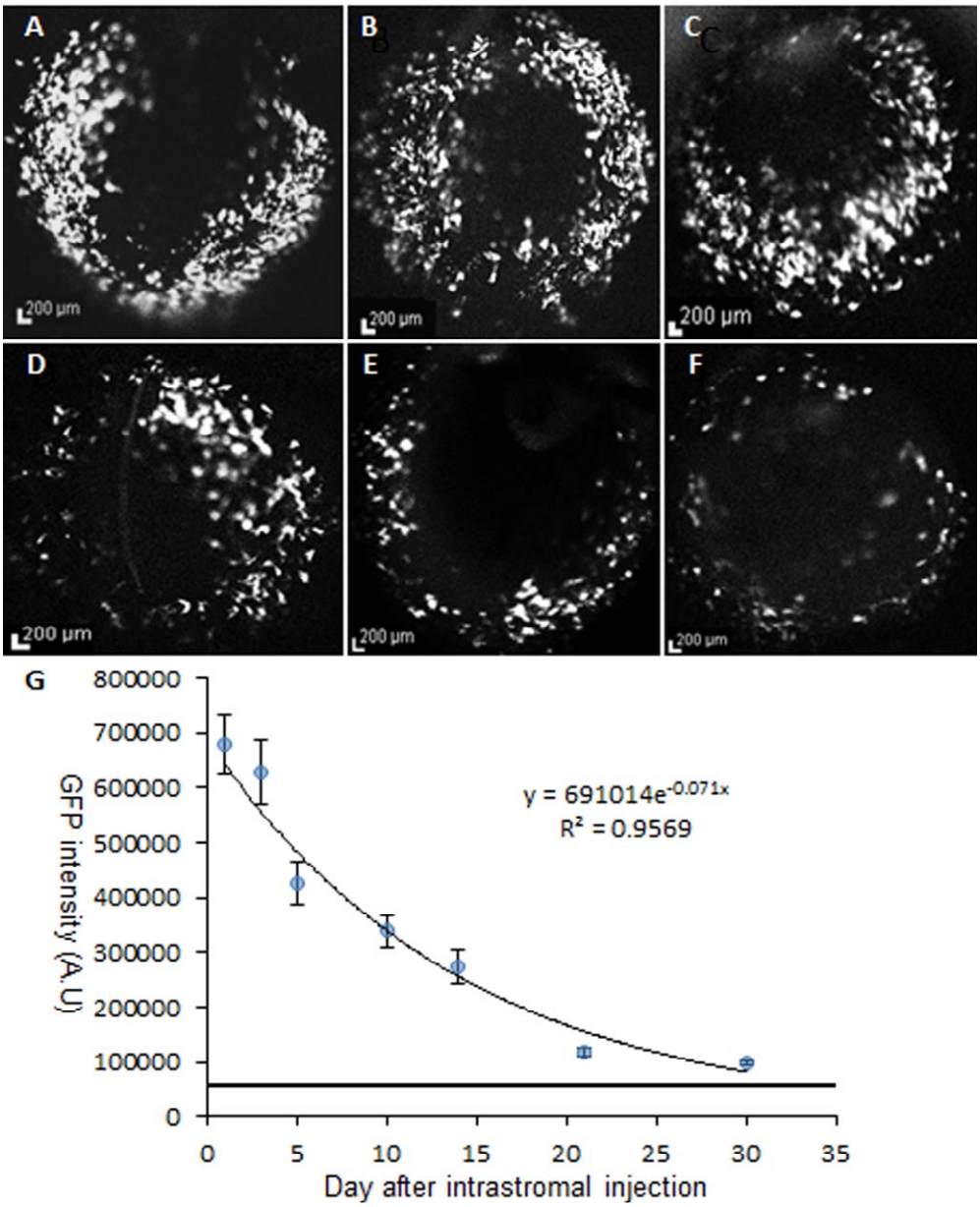

Figure 1. Intrastromal plasmids achieve GFP expression in cornea. (**A–F**) Images of cornea were taken by fluorescein angiography (488-nm laser; Spectralis) showing GFP expression time course. Representative corneas show GFP expression after corneal stroma injection of pCMV-GFP plasmid at 1 (**A**), 3 (**B**), 5 (**C**), 10 (**D**), 14 (**E**), and 21 (**F**) days. (**G**) Time course of GFP expression from day 1 to day 30. The fluorescence of GFP was calculated from the images by ImageJ software. Fitting curve was generated using $y = A\exp(B \times t)$. The half-life of GFP expression was calculated by the equation $y = 691014 \times e\text{^}-0.071 \times x$ where y = intensity, A (initial intensity value) = 691014, B (coefficient) = –0.071 and x (t) = time. Expression efficiency was measured by *white* intensity per pixel of corneas at the specific time points in a region of interest. Higher expression was observed on days 1 to 3, and it gradually decreased over time. Values are means ± SEM.

free EndoFree plasmid kit (Qiagen, Santa Clarita, CA, USA). Plasmids were sequenced to ensure fidelity and orientation. Purified shRNA plasmids were suspended in endotoxin-free Tris-EDTA (TE) buffer and injected into mouse corneal stroma.

Plasmid Injection

Under direct microscopic observation, a 30-gauge needle was used to nick the epithelium and anterior stroma of mouse cornea in the midperiphery. A 33-gauge needle on a 10-μL sterile gas-tight syringe (Hamilton Co., Reno, NV, USA) was introduced into the corneal stroma. A 2.5-μL (2-μg) dose of plasmid solution was injected into the stroma at 2 sites of the cornea for a total of 5 μL (4 μg).

Animals and Corneal Scarring Model

C57BL/6 female mice aged 12 to 16 weeks old were used in this study. The experiments were performed according to the Association for Research in Vision and Ophthalmology Statement on Use and Handling of Animals and were approved by the Institutional Animal Care and Use Committee of the University of Utah. Mice were anesthetized by intramuscular injection of ketamine (100 mg/kg) and xylazine

Investigative Ophthalmology & Visual Science

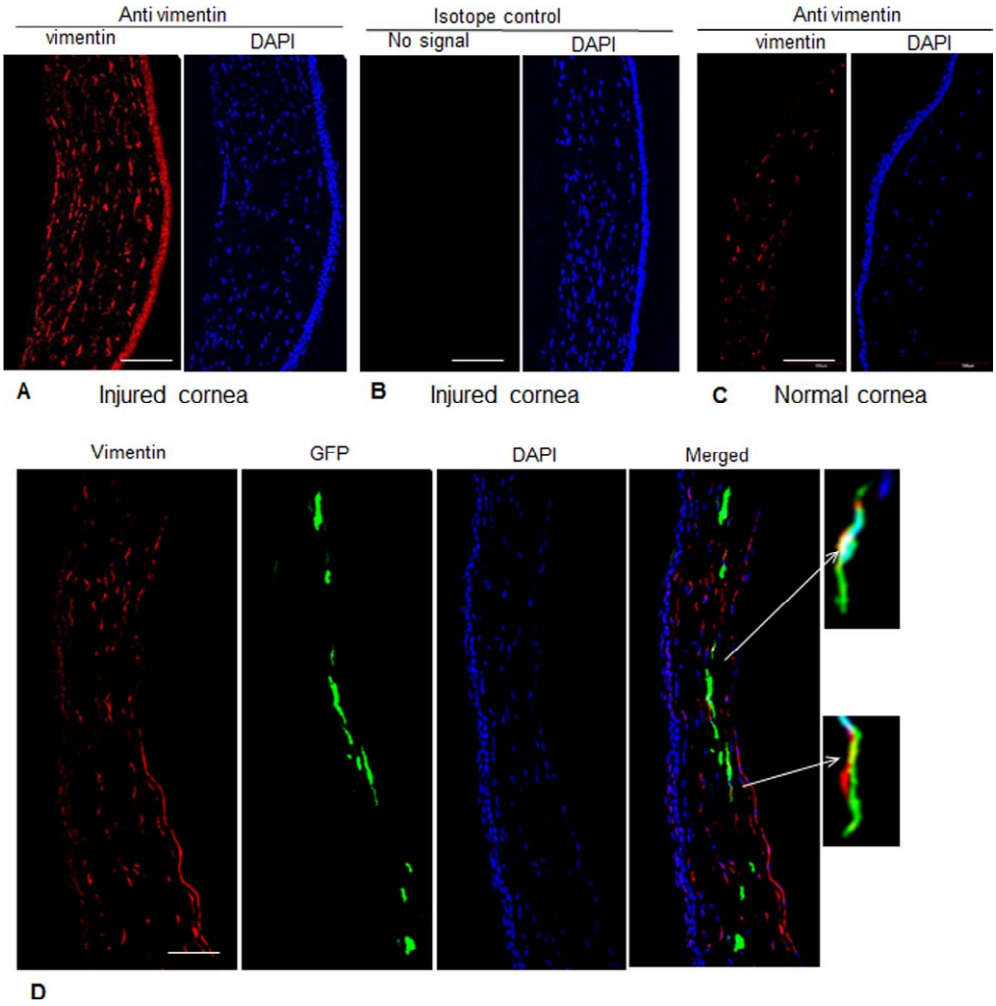

Figure 2. Vimentin is induced by injury. Immunohistochemistry of injured cornea (**A**, **B**), uninjured cornea (**C**), and pCMV-GFP injected cornea (**D**) sections (12 μm). Staining with anti-vimentin antibody in injured cornea showing vimentin expression in stroma and epithelial cells (**A**), lack of fluorescence with IgG control (**B**); pCMV-GFP-injected cornea showing vimentin and GFP expression in stroma, nuclear staining by DAPI, and merged image. (**D**) Extended part of merged image in stroma showing vimentin and GFP expression in stromal cell (keratocyte). *Scale bars*: 50 μm.

(10 mg/kg). The murine full-thickness incision model was developed in the central cornea to allow fibrotic repair with induction and differentiation of keratocytes into myofibroblasts. A 2-mm-long incision through the entire thickness (epithelium, stroma, and endothelium) was created in the central cornea, using a number 15 surgical blade (Bard-Parker, Caledonia, MI, USA). After incision, the wound was closed by means of two sutures placed equidistantly apart. After topical erythromycin ointment was applied, the mice were allowed to recover. In the corneal scarring model, the plasmid vectors and saline buffer were injected in the two sites of cornea at two time points. The first injection was given just before incision. The second plasmid injection was given before removal of the suture on postoperative day 8, followed by application of topical erythromycin ointment.

Grading of Corneal Opacity

On day 16, after the first injection, photographs of the mouse corneas were taken using a biomicroscope. Three masked observers graded the level of opacity in the cornea. Criteria for the level of opacity were grade 0, completely clear cornea; grade 1, faint corneal opacity; grade 2, mild opacity that was easily visible; grade 3, dense opacity that partially obscured iris details; and grade 4, severely dense opacity that completely obscured details of intraocular structures.

Green Fluorescent Protein In Vivo Imaging in Mouse Cornea

For in vivo imaging, we used the Spectralis laser (Heidelberg Engineering, Dossenheim, Germany) featuring a blue solid-state laser (wavelength, 488 nm) and barrier filter at 500 nm, which permits visualization of green fluorescent protein (GFP) expression in the cornea.[29] Using the fluorescein angiography (FA) camera mode and focusing the camera on the cornea, we acquired images using a Heidelberg retinal angiography-optical coherence tomography (HRA-OCT) at 1, 3, 5, 10, 14, 21, and 30 days after the injection of pCMV-GFP plasmid or controls. During imaging, a 55° lens was used to acquire wide-field images. Mice were anesthetized by intramuscular injection with ketamine (100 mg/kg) and xylazine (10 mg/kg). The white intensity per pixel of corneas at specific time points was calculated in a region of interest (ImageJ software; National Institutes of Health, Bethesda, MD, USA).

Investigative Ophthalmology & Visual Science

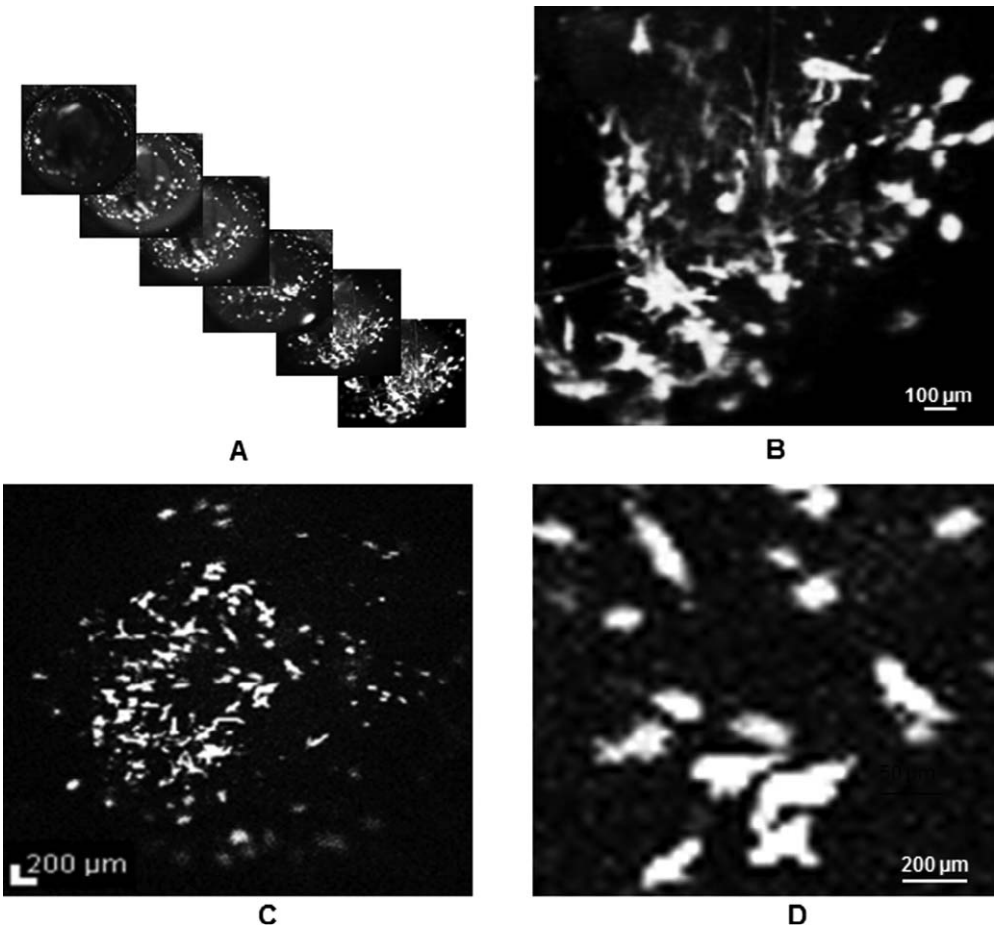

FIGURE 3. pCMV-GFP expression during wound healing. (**A**) Photomontage of GFP images in wounded cornea 3 days postinjection. (**B**) Extended figure of GFP expressing corneal fibroblast forming clusters of interconnected cells. (**C**) In contrast, unwounded corneal cells did not have interconnections. (**D**) Extended part of (**C**). Scale = 100 µm.

Staining of Mouse Cornea Section

Sixteen days after the first corneal injection the mice were euthanatized, and the corneas were excised and fixed with 4% formalin for 2 hours, treated with 15% sucrose for 2 hours, then treated with 30% sucrose solution overnight, and embedded in OCT medium (Tissue Tek; Sakura Finetek, Torrance, CA, USA) the next day. Histological examination of 12-µm sections was performed with hematoxylin-eosin (H&E) and Masson's trichrome staining. In Masson's trichrome blue staining represents collagen, and red staining represents cell cytoplasm and nuclei. To quantify fibrosis, we used ImageJ software. We calculated the number of highest intensity (blue) pixels and divided by the total number of pixels per corneal section in each treatment groups. The number of highest intensity pixels and total pixels per image were calculated by ImageJ histogram. We removed zero- and 1-intensity pixels from the data set as these were considered background. For immunofluorescence, frozen sections (12 µm) were blocked with 5% (w/v) fetal bovine serum (FBS) in phosphate-buffered saline/tween PBST. The sections were probed with anti-rabbit vimentin (1:200 dilution; Abcam, Cambridge, MA, USA) and mouse anti-α-SMA (1:400 dilution; Sigma-Aldrich, St. Louis, MO, USA) conjugated with Cy3 overnight at 4°C. The secondary antibody Alexa Fluor 488 goat anti-rabbit immunoglobulin G (IgG) or Alexa Fluor 546 goat anti-rabbit IgG (Life Technologies) was used at 1:3000 dilution for 1 hour. Nuclei were stained with 4′, 6-diamidino-2-phenylindole (DAPI) and mounted with medium for fluorescence. Photos were taken with confocal microscopy.

Real-Time PCR and Western Blotting for Vimentin From Corneal Tissue

Ten days after injection, the corneas of mice treated with shRNA plasmid injections were harvested. Total RNA from these samples was extracted with RNeasy mini-kit with DNase I treatment (Qiagen). cDNAs were synthesized from 500 ng total RNA, using the Omniscript RT kit (Qiagen) and oligo(dT) primer (dT20; Life Technologies) according to the manufacturer's instructions. Real-time PCR for vimentin was performed using the QuantiTect SYBR Green PCR kit (Qiagen) and 1 µL cDNA. Real-time PCR conditions were 95°C for 10 minutes, followed by 40 cycles of 94°C for 15 seconds, 55°C for 30 seconds, and 72°C for 30 seconds. For Western blotting of vimentin, each cornea was freeze-fractured in liquid nitrogen, dissolved in radioimmunoprecipitation assay buffer by sonication, and subjected to SDS-PAGE under reducing conditions. A total of 10 µg of protein lysate per lane was loaded. Blotting was conducted on polyvinylidene fluoride membranes (Millipore, Billerica, MA, USA). Primary antibody anti-rabbit vimentin (1:1000 dilution; Abcam) incubation was done overnight at 4°C, followed by incubation with secondary horseradish-peroxidase (HRP)-linked anti-rabbit antibodies for 1 hour at room temperature. Secondary HRP antibodies were detected

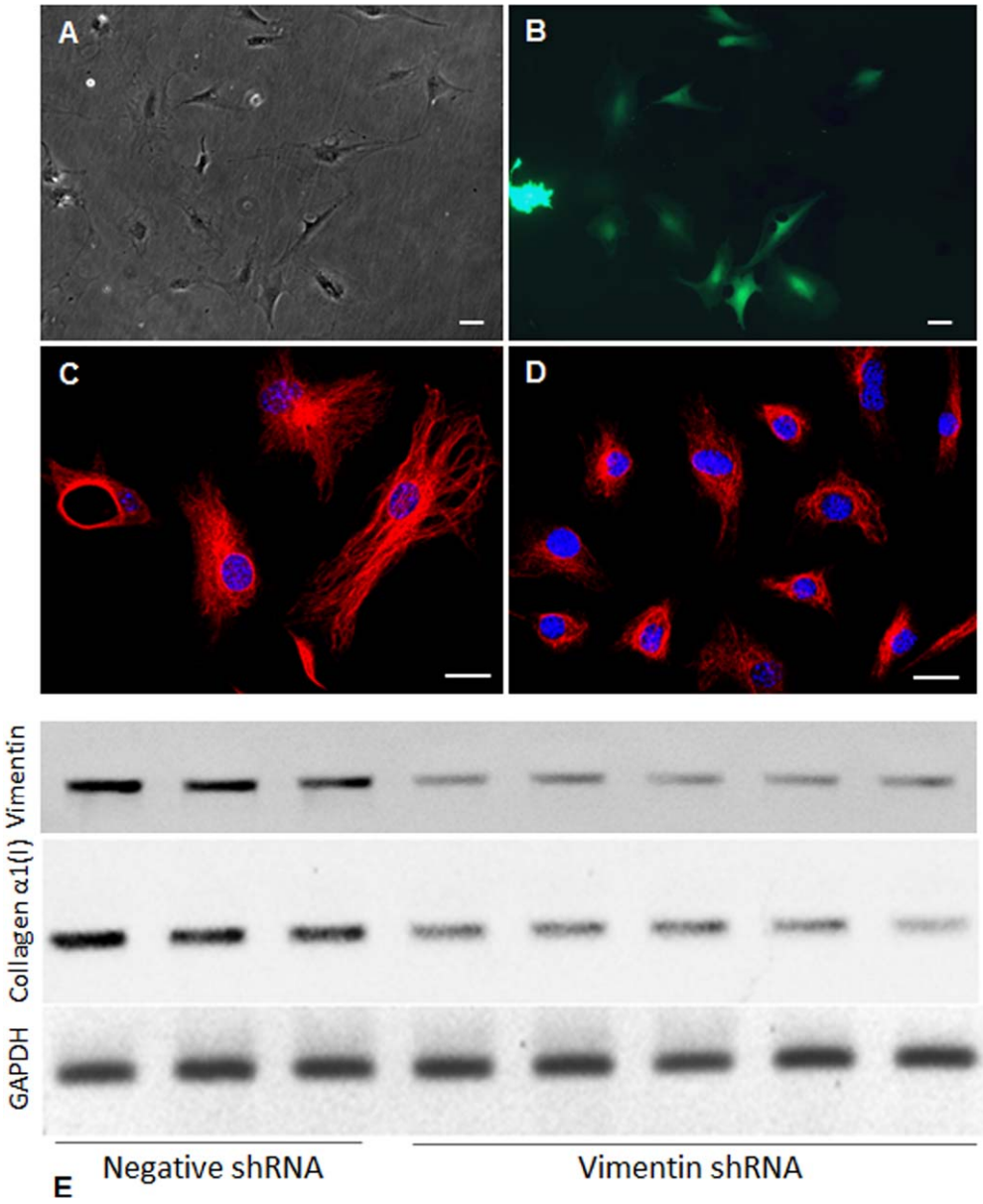

Figure 4. Vimentin shRNA reduces filament formation in primary mouse corneal fibroblasts. (**A**) Brightfield microscopy of (**B**). (**B**) Primary corneal fibroblasts transfected with pCMV-GFP plasmid. (**C**) Transfection with pshRNA.neg showing extended vimentin filament, and (**D**) transfection with pshRNA.vim showing smaller filaments. *Scale bar*: 20 μm. (**E**) RT-PCR results showing mRNA expression in shRNA plasmid transfected mouse corneal fibroblast. Vimentin and collagen a1(I) mRNA are visibly reduced in pshRNA.vim compared to pshRNA.neg (multiple samples of the same preparation).

using chemiluminescence detection solution (Life Technologies). For normalization, GAPDH signal was used.

Isolation of Mouse Corneal Fibroblasts Primary Cultures, Plasmid Transfection, RT-PCR, and Immunostaining

Six mouse corneas were aseptically harvested, washed with minimum essential medium (Life Technologies), subsectioned into small pieces, and placed in tissue culture plates containing Dulbecco's modified Eagle's medium (DMEM; Life Technologies) and 10% FBS to obtain corneal fibroblasts (CFs). CFs were then incubated in a humidified 5% CO_2 incubator at 37°C. In approximately 7 to 10 days, fibroblasts began migrating from the stromal fragments. Once the primary culture reached 90% confluence, the stromal subsections were removed by forceps. The confluent cells were trypsinized and replated on 60-mm tissue culture plates in DMEM containing 10% FBS and maintained in the same medium. Plasmids were delivered by nucleofection (Amaxa, Gaithersburg, MD, USA) using Basic Nucleofector kit (Lonza, Basel, Switzerland). For one nucleofection, 1×10^6 cells were used and grown on a 6-well plate for RT-PCR. The transfected cells were also cultured in collagen-coated coverslips. pCMV-GFP plasmid was transfected to assess for efficiency. After 72 hours, cells were harvested to isolate total RNA, and coverslips were rinsed with PBS, fixed with 4% formaldehyde for 15 minutes, and made permeable with 0.05% Triton X-100 for 10 minutes; then, cells were blocked with 5% FBS in PBST for 1 hour at room temperature, incubated with anti-vimentin antibody (1:200 dilution; Abcam) in PBST contain-

Investigative Ophthalmology & Visual Science

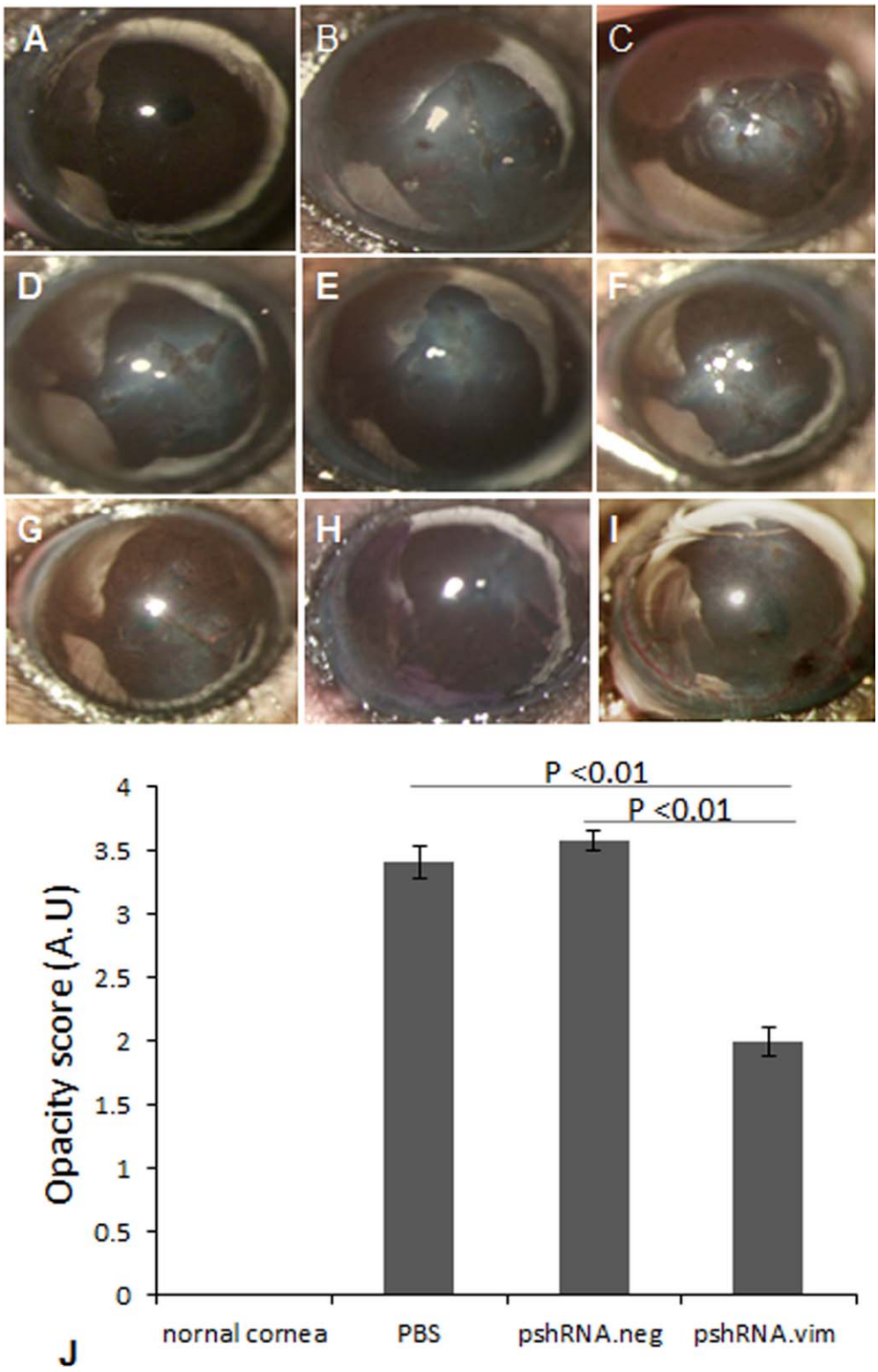

Figure 5. Vimentin shRNA improves corneal clarity after injury. Mice were subjected to corneal injury and treated with PBS, pshRNA.neg, or pshRNA.vim by intrastromal injection at 2 time points (days 1 and 8). Representative images at 16 days after first injection show dramatic reduction of corneal opacification in pshRNA.vim treated cornea (**G**, **H**, **I**) compared to PBS and pshRNA.neg-treated corneas (**B–F**). A, unwounded normal cornea. (**J**) Quantification of corneal opacity seen by biomicroscopy at day 16, using opacity scale of 0 (clear) to 4 (opaque) ($n = 12$ eyes in PBS; $n = 12$ eyes in pshRNA.neg; $n = 20$ eyes in pshRNA.vim group). Values are means ± SEM. *P* value was calculated by *U* test.

Investigative Ophthalmology & Visual Science

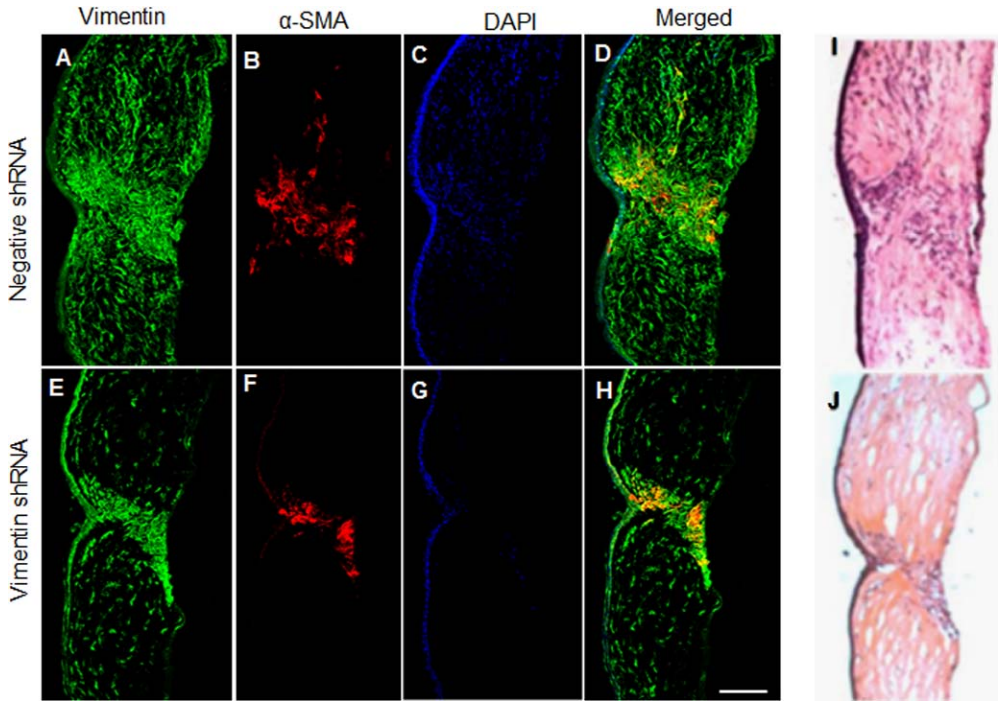

FIGURE 6. Vimentin shRNA reduced vimentin and α-SMA expression in wounded mouse cornea section 16 days after shRNA treatment. Cell nuclei are stained *blue* with DAPI; SMA-positive cells are stained *red*; vimentin-positive cells are stained *green*. Vimentin-positive cells around the wound's edge represent a cell subpopulation with high cell density and high vimentin expression in shRNA.neg plasmid, whereas this was greatly reduced in shRNA.vim plasmid treatment. α-SMA is also reduced in shRNA.vim treatment compared to negative control. H&E staining of shRNA.neg-treated cornea section (**I**) and shRNA.vim-treated cornea (**J**). *Scale bar*: 100 μm.

ing 5% FBS overnight at 4°C, washed with PBS five times, and incubated with the secondary antibody Alexa Fluor 488 goat anti-rabbit IgG (1:3000 dilution; Life Technologies) for 1 hour at room temperature. After being washed with PBS, coverslips were mounted with medium containing DAPI and analyzed with confocal microscopy. cDNAs were synthesized as described above. The PCR condition was 95°C for 3 minutes, followed by 25 cycles of 94°C for 15 seconds, 55°C for 30 seconds, and 72°C for 30 seconds, and a final 7-minute extension.

RESULTS

Time Course of GFP Expression

Initial studies were aimed at determining the duration of naked plasmid (pCMV-GFP) expression in mouse corneal keratocytes in vivo. We delivered a total of 4 μg of pCMV-GFP plasmid (suspended in 5 μL of normal saline, 2.5 μL for each injection) by intrastromal injection into two (inferior and superior) sites of the cornea. GFP fluorescence was assayed in vivo on days 1, 3, 5, 10, 14, 21, and 30 after plasmid injection by capturing images with the Spectralis laser (Heidelberg); fluorescent intensity per pixel was calculated. The expression of GFP was highest between 1 and 3 days and gradually declined over time. We observed that prominent GFP expression lasted up to day 15 and was detectable up to 21 days (Fig. 1). On day 30, much less GFP expression was detectable. Figure 1G shows the time course of GFP expression. We calculated the half-life of plasmid expression to be approximately 10 days.

Histological Finding of GFP in Corneal Stroma

To investigate the localization of GFP expression, immunohistochemistry of 12-μm corneal sections stained with anti-vimentin antibody and DAPI staining was performed. Fluorescence microscopy examination of the sections showed that GFP was present in the spindle-shaped cells of the corneal stroma. These cells also stained positive for vimentin; therefore, we speculated these spindle-shaped cells were keratocytes (Fig. 2D). GFP was not detected in other corneal cells, nor was it detectable in sections from control corneas. The injured cornea showed vimentin expression in spindle-shaped stromal and epithelial cells (Fig. 2A). There was no fluorescence in IgG-containing control (Fig. 2B). The uninjured cornea section demonstrated vimentin expression only in the spindle-shaped stromal cells (Fig. 2C).

In Vivo GFP Expression in Wounded Versus Unwounded Cornea

To investigate the localization of GFP expression in a wounded cornea, we injected pCMV-GFP plasmid into two sites of the mouse cornea. Five minutes after the injection, we made a partial-thickness incision into the central cornea to mimic corneal injury. Confocal microscopy analysis using the Spectralis laser was performed on day 3 postinjury. The data demonstrated that transfected cells were localized to the fibrotic regions around the incision. Cell clusters varied in number from 3 to 10 cells. They appeared to maintain contact with each other via extended dendritic processes. At higher magnification, the transfected cells appeared as broad, flattened cells with extensions to adjacent cells (Figs. 3A, 3B). The GFP-expressing cells in the unwounded cornea did not show cell clusters or extended dendritic processes; rather, they were elliptical and separated from one another (Figs. 3C, 3D). Based on these observations, it can be speculated that the broad, flattened cells are activated fibroblasts induced in the

Investigative Ophthalmology & Visual Science

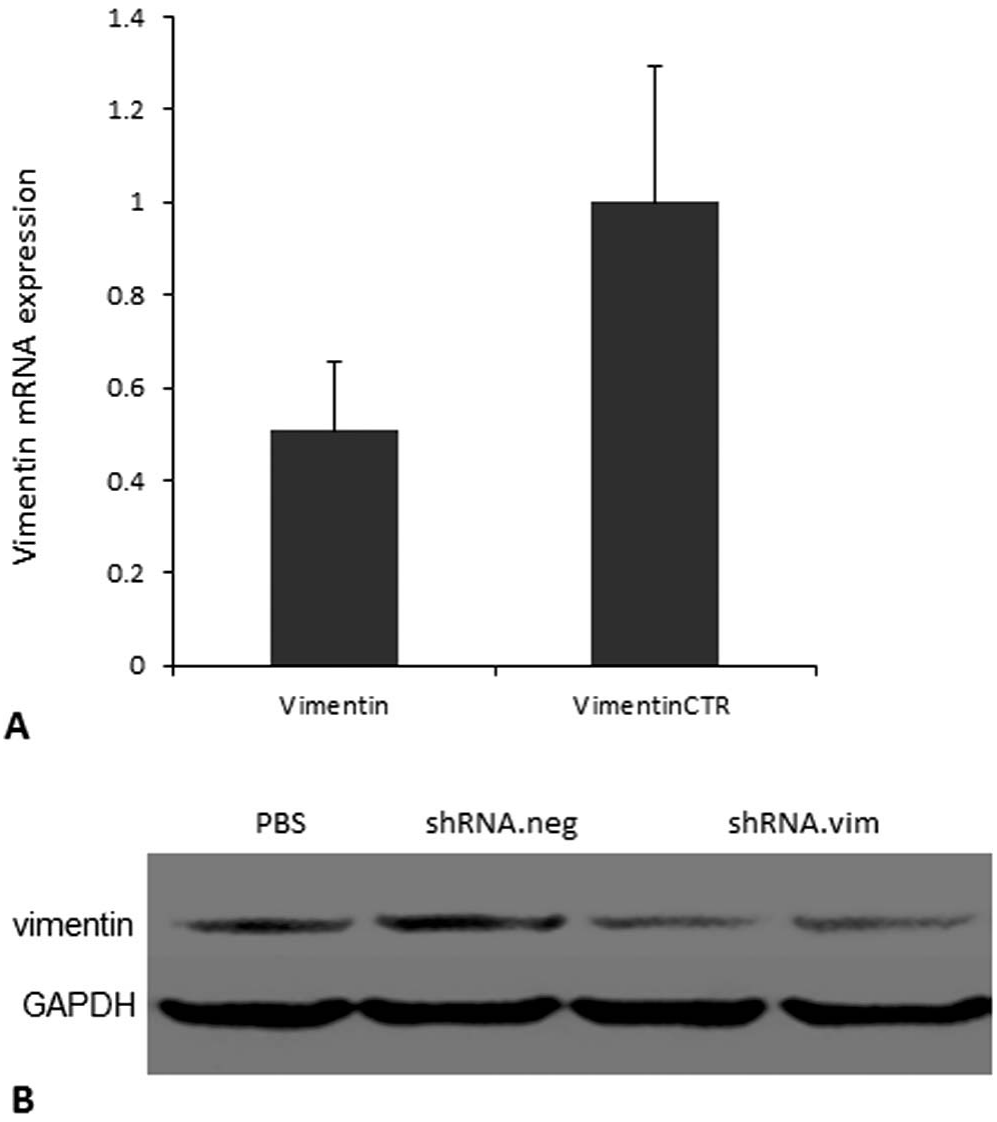

Figure 7. shRNA.vim knocks down vimentin expression on real-time PCR (**A**) and Western blot (**B**) analyses. A significant decrease of vimentin was observed in shRNA.vim-delivered cornea compared to that in controls. Results were normalized by GAPDH. In real-time PCR ($n = 6$ in each group), error bar is ± SD, $P < 0.05$, calculated by 2-tailed Student's *t*-test.

postinjury model, whereas the elliptical cells in unwounded cornea model are keratocytes.

In Vitro Vimentin shRNA Blocks Filamentous Network Formation of Vimentin in Primary Mouse Corneal Fibroblasts and Collagen I Expression

To evaluate the inhibitory effects of vimentin shRNA plasmid (pshRNA.vim) compared to negative shRNA plasmid (pshRNA.neg), we used a primary culture of mouse corneal keratocytes in DMEM with 10% FBS to promote differentiation of keratocytes into fibroblasts.[30] We then performed in vitro transfection with each plasmid. After the plasmid transfection, the cells were immunostained for anti-vimentin antibody. As shown in Figures 4C and 4D, pshRNA.vim inhibited the normal formation of the vimentin filament network. The network developed perinuclear formations in contrast to the expected extending filamentous structure. RT-PCR of pshRNA.vim-transfected CFs showed reduction of expression of both the mRNA of vimentin and collagen type I (Fig. 4E).

In Vivo Vimentin shRNA in a Wounded Mouse Cornea Model Inhibited Scarring

To study in vivo fibrosis, we used an injury model of incision followed by suture placement in the central cornea of mice. We injected plasmids at two time points: on the day of injury and on day 8. On day 16 postinjury, corneal opacity was assessed by examining stereomicroscopy images. Figure 5J shows the mean opacity scores of the corneas treated with pshRNA.vim, pshRNA.neg, and PBS. The controls (PBS and pshRNA.neg) showed prominent fibrosis in the cornea as manifested by opacification. The pshRNA.neg and PBS-injected corneas showed average mean ± SEM opacity scores of 4.1 ± 0.11 and 3.42 ± 0.13, respectively. In contrast, the injured corneas treated with pshRNA.vim demonstrated a substantial decrease in corneal fibrosis (corneal opacity score of 2 ± 0.12).

Vimentin knockdown in the injured mouse cornea was confirmed by real-time PCR and Western blot analysis (Fig. 7). We then immunostained the sections with anti-vimentin

Investigative Ophthalmology & Visual Science

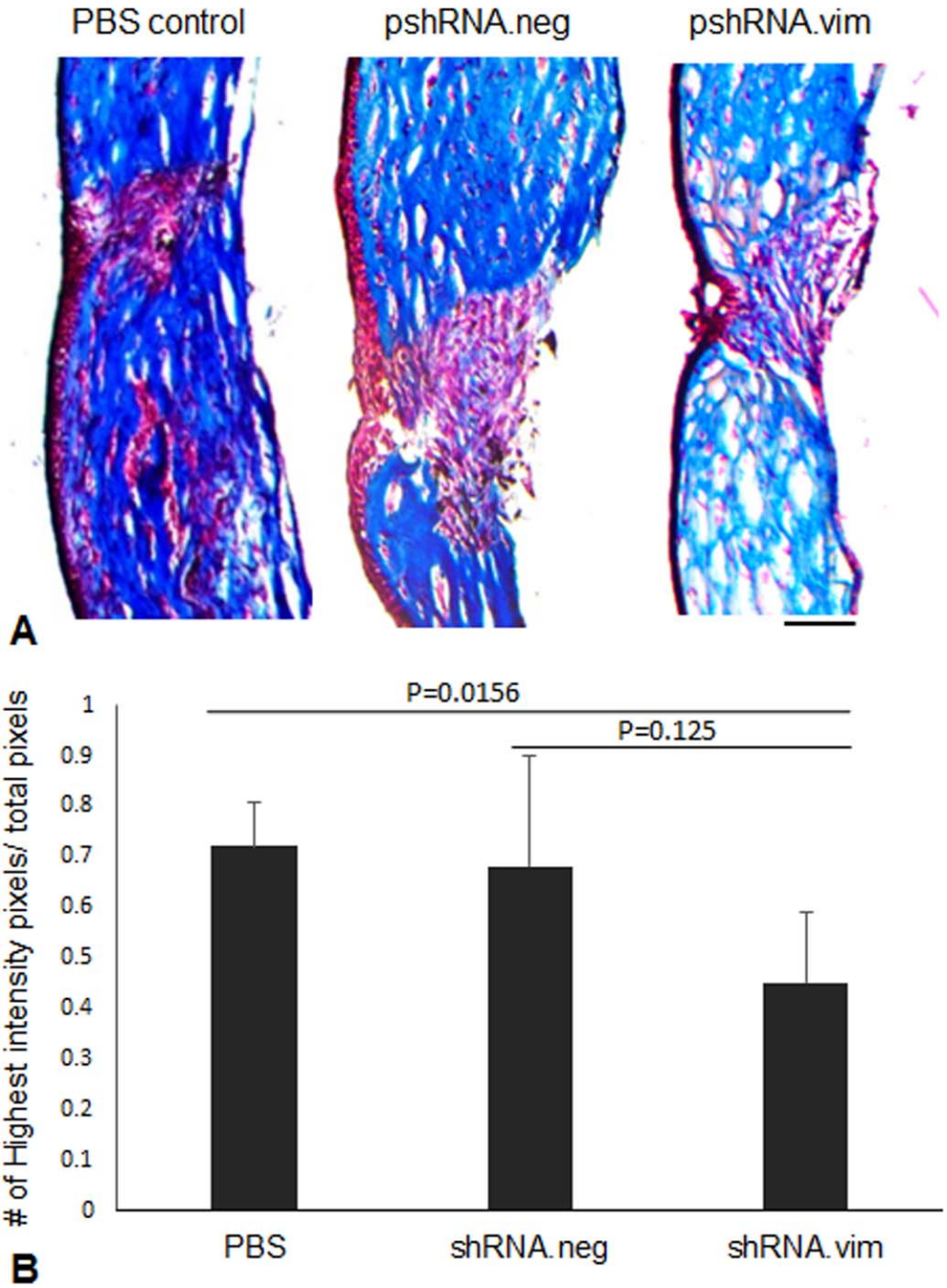

FIGURE 8. Sample stained with Masson's trichrome technique. Representative pshRNA.vim treatment reduced collagen (*blue*) in stroma around wounding in comparison to PBS and pshRNA.neg on day 16. Cell cytoplasm and nuclei are stained *red*. *Scale bar*: 100 μm. (**B**) Quantification of fibrosis scoring for *trichrome-stained* corneal sections ($n = 4$ per group).

antibody and anti-αSMA antibody to assess wound contraction. The stained sections showed that cells around the wound edges represented a subpopulation of cells with greater density and greater vimentin expression in the control cornea (PBS injection) than in corneas treated with pshRNA.vim. Corneal thicknesses of treated sections were 132 μm compared with 171 μm in untreated sections. Taken together, these findings indicate that the pshRNA.vim treatment decreased injury-induced vimentin cell density, cell migration toward the incision site, and α-SMA expression (Fig. 6). Masson's trichrome staining showed a decrease of blue color at the stroma near the incision, indicating there was less collagen formation in the pshRNA.vim-treated injured corneas (Fig. 8).

DISCUSSION

Nonviral gene delivery or application of naked plasmid DNA is a simple, safe, and effective delivery method with no inflammatory response.[12,31] The viral vector-mediated method also is an effective way of gene transfer[8–11]; however, this type of gene transduction method often induces unwanted inflammation.[30–33] Considering that minimal inflammation in the

cornea can cause serious adverse effects, nonviral gene delivery is a desirable method of gene transfection. In this study, we successfully transfected the pCMV-GFP plasmid into the corneal stroma using two injection sites. Prominent GFP expression was detected at 15 days, and slight expression was detectable up to 21 days. In a different study, pCMV-driven LacZ plasmid in intrastromal injection persisted for 10 days.[12] Oshima et al.[34] reported that plasmid DNA transfection to rat corneal stroma was achieved by a combination of corneal injection and application of electric pulses. In that study, expression of the GFP gene peaked at 6 days and persisted until day 15 with a 5-μL solution of corneal injection containing 2.5 μg of plasmid. Oshima et al.[35] also reported that LacZ gene expression was detectable in corneal endothelium for at least 21 days, using the same technique. In our study, the longer duration of GFP expression (half-life of plasmid expression of approximately day 10) may be attributed to an increased amount (total of 4 μg) of plasmid DNA delivery by injection in two sites of cornea.

In our study, we demonstrated that injured mouse corneal cells were successfully transfected by pCMV-GFP plasmid. In injured corneas, the GFP-positive cells showed extensive dendritic-like processes which extended to adjacent cells, the morphology of which suggested a transition from keratocytes to fibroblasts. These dendritic extensions were absent in uninjured corneas. Previous studies have suggested that wound healing fibroblasts of rabbit corneas showed similar dendrite-activated cells when transduced by the oncoretrovirus vector RD114.[36]

We demonstrate that in vivo vimentin knockdown using pshRNA.vim with two intracorneal injections inhibited the fibrotic response to corneal incision injury, reduced opacity, and therefore restored corneal clarity. Reduction of fibrosis may improve endothelial pump function as noted by reduced edema in vivo. Immunostaining of corneal stroma in pshRNA.neg-treated cornea demonstrated that the cells around the wound edges have a higher cell density and a higher vimentin expression compared to pshRNA.vim plasmid treatment. This suggests that vimentin promotes cell migration as well as proliferation. Fibroblast migration was decreased in wound healing in both vimentin-deficient mice and in an in vitro model after vimentin knockdown.[26–28] In addition, the immunostaining with αSMA demonstrated decreased myofibroblast formation at the injury site of pshRNA.vim-treated cornea. α-SMA is known to be upregulated in myofibroblasts which secrete ECM to promote wound healing.[37] This suggests that vimentin knockdown reduced cell migration and proliferation, in turn reducing myofibroblast differentiation at the injury site. Quantification of Masson's trichrome staining in wounded corneal model showed reduced collagen at the stroma near the incision, suggesting vimentin knockdown delayed wound contracture.[24,25]

Future studies should explore the effect of vimentin knockdown on endothelial wound repair and barrier integrity. In addition, these studies should assess whether wound strength is compromised by vimentin knockdown. It can be deduced from our data that vimentin downregulation by shRNA treatment may play a beneficial role in reducing fibroblast transformation and opacification in corneal wound healing.

Acknowledgments

We thank Tadashi Miya, and Christina Mamalis for technical support. The authors alone are responsible for the content and writing of the paper.

Supported in part by an unrestricted grant from Research to Prevent Blindness, Inc. (New York, NY, USA) to the Department of Ophthalmology & Visual Sciences, University of Utah, and National Institutes of Health NEI Grant 5R01EY017950.

Disclosure: **S.K. Das**, None; **I. Gupta**, None; **Y.K. Cho**, None; **X. Zhang**, None; **H. Uehara**, None; **S.K. Muddana**, None; **A.A. Bernhisel**, None; **B. Archer**, None; **B.K. Ambati**, None

References

1. Foster A, Resnikoff S. The impact of Vision 2020 on global blindness. *Eye (Lond)*. 2005;19:1133–1135.
2. Congdon N, O'Colmain B, Klaver CC, Klein R, Munoz B, Friedman DS, et al. Causes and prevalence of visual impairment among adults in the United States. *Arch Ophthalmol*. 2004;122:477–485.
3. Hassell JR, Birk DE. The molecular basis of corneal transparency. *Exp Eye Res*. 2010;91:326–335.
4. Qazi Y, Wong G, Monson B, Stringham J, Ambati BK. Corneal transparency: genesis, maintenance and dysfunction. *Brain Res Bull*. 2010;81:198–210.
5. Wilson SE, Mohan RR, Ambrosio R Jr, Hong J, Lee J. The corneal wound healing response: cytokine-mediated interaction of the epithelium, stroma, and inflammatory cells. *Prog Retin Eye Res*. 2001;20:625–637.
6. Seiler T, McDonnell PJ. Excimer laser photorefractive keratectomy. *Surv Ophthalmol*. 1995;40:89–118.
7. Netto MV, Mohan RR, Ambrosio R Jr, Hutcheon AE, Zieske JD, Wilson SE. Wound healing in the cornea: a review of refractive surgery complications and new prospects for therapy. *Cornea*. 2005;24:509–522.
8. Mohan RR, Sharma A, Netto MV, Sinha S, Wilson SE. Gene therapy in the cornea. *Prog Retin Eye Res*. 2005;24:537–559.
9. Mohan RR, Tandon A, Sharma A, Cowden JW, Tovey JC. Significant inhibition of corneal scarring in vivo with tissue-selective, targeted AAV5 decorin gene therapy. *Invest Ophthalmol Vis Sci*. 2011;52:4833–4841.
10. Sharma A, Ghosh A, Siddapa C, Mohan RR. Gene therapy for the cornea, conjunctiva, and lacrimal gland. In: Besharse J, Dana R, Dartt DA, eds. *Encyclopedia of the Eye*. Amsterdam: Elsevier Academic Press; 2010;185–194.
11. Hao J, Li SK, Kao WW, Liu CY. Gene delivery to cornea. *Brain Res Bull*. 2010;81:256–261.
12. Sharma A, Ghosh A, Hansen ET, Newman JM, Mohan RR. Transduction efficiency of AAV 2/6, 2/8 and 2/9 vectors for delivering genes in human corneal fibroblasts. *Brain Res Bull*. 2010;81:273–278.
13. Stechschulte SU, Joussen AM, von Recum HA, Poulaki V, Moromizato Y, Yuan J, et al. Rapid ocular angiogenic control via naked DNA delivery to cornea. *Invest Ophthalmol Vis Sci*. 2001;42:1975–1979.
14. Williams KA, Coster DJ. Gene therapy for diseases of the cornea—a review. *Clin Experiment Ophthalmol*. 2010;38:93–103.
15. Shayakhmetov DM, Di Paolo NC, Mossman KL. Recognition of virus infection and innate host responses to viral gene therapy vectors. *Mol Ther*. 2010;18:1422–1429.
16. Thomas CE, Ehrhardt A, Kay MA. Progress and problems with the use of viral vectors for gene therapy. *Nat Rev Genet*. 2003;4:346–358.
17. Yang Y, Nunes FA, Berencsi K, Furth EE, Gonczol E, Wilson JM. Cellular immunity to viral antigens limits E1-deleted adenoviruses for gene therapy. *Proc Natl Acad Sci U S A*. 1994;91:4407–4411.
18. Jester JV, Petroll WM, Cavanagh HD. Corneal stromal wound healing in refractive surgery: the role of myofibroblasts. *Prog Retin Eye Res*. 1999;18:311–356.

19. Tandon A, Tovey JC, Sharma A, Gupta R, Mohan RR. Role of transforming growth factor Beta in corneal function, biology and pathology. *Curr Mol Med*. 2010;10:565–578.
20. West-Mays JA, Dwivedi DJ. The keratocyte: corneal stromal cell with variable repair phenotypes. *Int J Biochem Cell Biol*. 2006;38:1625–1631.
21. Wilson SE, Chaurasia SS, Medeiros FW. Apoptosis in the initiation, modulation and termination of the corneal wound healing response. *Exp Eye Res*. 2007;85:305–311.
22. Zieske JD, Guimaraes SR, Hutcheon AE. Kinetics of keratocyte proliferation in response to epithelial debridement. *Exp Eye Res*. 2001;72:33–39.
23. Helfand BT, Mendez MG, Murthy SN, Shumaker DK, Grin B, Mahammad S, et al. Vimentin organization modulates the formation of lamellipodia. *Mol Biol Cell*. 2011;22:1274–1289.
24. Eckes B, Colucci-Guyon E, Smola H, Nodder S, Babinet C, Krieg T, et al. Impaired wound healing in embryonic and adult mice lacking vimentin. *J Cell Sci*. 2000;113(pt 13):2455–2462.
25. Eckes B, Dogic D, Colucci-Guyon E, Wang N, Maniotis A, Ingber D, et al. Impaired mechanical stability, migration and contractile capacity in vimentin-deficient fibroblasts. *J Cell Sci*. 1998;111(pt 13);1897–1907.
26. Rogel MR, Soni PN, Troken JR, Sitikov A, Trejo HE, Ridge KM. Vimentin is sufficient and required for wound repair and remodeling in alveolar epithelial cells. *FASEB J*. 2011;25:3873–3883.
27. Chaurasia SS, Kaur H, de Medeiros FW, Smith SD, Wilson SE. Dynamics of the expression of intermediate filaments vimentin and desmin during myofibroblast differentiation after corneal injury. *Exp Eye Res*. 2009;89:133–139.
28. Ishizaki M, Zhu G, Haseba T, Shafer SS, Kao WW. Expression of collagen I, smooth muscle alpha-actin, and vimentin during the healing of alkali-burned and lacerated corneas. *Invest Ophthalmol Vis Sci*. 1993;34:3320–3328.
29. Wang J, Shousha MA, Perez VL, Karp CL, Yoo SH, Shen M, et al. Ultra-high resolution optical coherence tomography for imaging the anterior segment of the eye. *Ophthalmic Surg Lasers Imaging Retina*. 2011;42:S15–S27.
30. Jester JV, Barry PA, Lind GJ, Petroll WM, Garana R, Cavanagh HD. Corneal keratocytes: in situ and in vitro organization of cytoskeletal contractile proteins. *Invest Ophthalmol Vis Sci*. 1994;35:730–743.
31. Buss DG, Giuliano EA, Sharma A, Mohan RR. Isolation and cultivation of equine corneal keratocytes, fibroblasts, and myofibroblasts. *Vet Ophthalmol*. 2010;13:37–42.
32. Huang X, Yang Y. Innate immune recognition of viruses and viral vectors. *Hum Gene Ther*. 2009;20:293–301.
33. Tang DC, DeVit M, Johnston SA. Genetic immunization is a simple method for eliciting an immune response. *Nature*. 1992;356:152–154.
34. Wolff JA, Malone RW, Williams P, Chong W, Acsadi G, Jani A, et al. Direct gene transfer into mouse muscle in vivo. *Science*. 1990;247:1465–1468.
35. Oshima Y, Sakamoto T, Hisatomi T, Tsutsumi C, Sassa Y, Ishibashi T, et al. Targeted gene transfer to corneal stroma in vivo by electric pulses. *Exp Eye Res*. 2002;74:191–198.
36. Gatlin J, Melkus MW, Padgett A, Petroll WM, Cavanagh HD, Garcia JV, et al. In vivo fluorescent labeling of corneal wound healing fibroblasts. *Exp Eye Res*. 2003;76:361–371.
37. Hinz B, Phan SH, Thannickal VJ, Galli A, Boachaton-Piallat M, Gabbiani G. The myofibroblast. *Am J Pathol*. 2007;170:1807–1816.

Investigative Ophthalmology & Visual Science